Ultrasonics 50 (2010) 202–207

Contents lists available at ScienceDirect

Ultrasonics

journal homepage: www.elsevier.com/locate/ultras

Picosecond acoustics in vegetal cells: Non-invasive *in vitro* measurements at a sub-cell scale

B. Audoin [a,*], C. Rossignol [a], N. Chigarev [a], M. Ducousso [a], G. Forget [b], F. Guillemot [b], M.C. Durrieu [b]

[a] Université de Bordeaux, CNRS, UMR 5469, Talence F-33405, France
[b] Université de Bordeaux, INSERM, UMR 577, Bordeaux F-33000, France

ARTICLE INFO

Article history:
Received 22 July 2009
Received in revised form 11 September 2009
Accepted 14 September 2009
Available online 27 September 2009

PACS:
43.35
43.80
43.20

Keywords:
Acoustic microscopy
Biophononics
Cell imaging
Medical applications
Picosecond acoustics

ABSTRACT

A 100 fs laser pulse passes through a single transparent cell and is absorbed at the surface of a metallic substrate. Picosecond acoustic waves are generated and propagate through the cell in contact with the metal. Interaction of the high frequency acoustic pulse with a probe laser light gives rise to Brillouin oscillations. The measurements are thus made with lasers for both the opto-acoustic generation and the acousto-optic detection, and acoustic frequencies as high as 11 GHz can be detected, as reported in this paper. The technique offers perspectives for single cell imaging. The in-plane resolution is limited by the pump and probe spot sizes, i.e. ~1 μm, and the in-depth resolution is provided by the acoustic frequencies, typically in the GHz range. The effect of the technique on cell safety is discussed. Experiments achieved in vegetal cells illustrate the reproducibility and sensitivity of the measurements. The acoustic responses of cell organelles are significantly different. The results support the potentialities of the hypersonic non-invasive technique in the fields of bio-engineering and medicine.

1. Introduction

The laser–ultrasonic techniques, in which ultrasonic waves are both generated and detected with laser light, are receiving growing attention because of their wide range of applicability in non-destructive control and evaluation. These techniques are particularly well suited for material characterisation when measurements must be made without contacting or applying coupling gel to the structure. Moreover, since the duration of the laser pulse can be very short, high resolution in space (nm in-depth) and time (ps) can be achieved.

Femtosecond laser pulses have been used, since the end of the 80s, to perform generation and detection of longitudinal acoustic waves in sub-micrometric films, multilayers structures and other nanostructures [1]. Ultrafast ultrasonic technique consists in measuring the transient reflectivity changes induced in a structure by the propagation of an optically generated acoustic wave. The absorption of a light pulse, namely the pump pulse, sets up a local thermal stress. This stress generates an elastic strain pulse propagating through the sample. The acoustic perturbation induces a change in the optical reflectivity of the structure. The reflectivity change is probed by a transient reflectometric or interferometric detection [2].

The main application fields of ultrafast opto-acoustics today are solid state physics and micro electronics. The latter is requiring an accurate mean of measuring the thicknesses and of controlling the bonding at a nanometer scale, that is provided by the picosecond acoustic technique.

Despite recent development of femtosecond photothermal techniques in the field of biology, no application of picosecond acoustics has concerned this field up to now. However picosecond acoustics offers promising potentialities for biological imaging in the immediate future. Recently, measurement of high frequency acoustic waves generated with femtosecond lasers were performed by other teams in water [3] and liquid mercury [4]. We have recently reported on preliminary measurements (5–10 GHz) performed on vegetal cells [5].

The Section 2 of this paper presents the picosecond photoacoustic generation in a cell. Then a one dimension model, Section 3, accounting for photothermal generation, thermo-acoustic coupling and acousto-optic detection allows to predict the measured

* Corresponding author. Address: Laboratoire de Mécanique Physique, Université Bordeaux 1, 351 Cours de la Libération, F-33405 Talence, France. Tel.: +33 5 40 00 69 69; fax: +33 5 40 00 69 64.
E-mail address: b.audoin@lmp.u-bordeaux1.fr (B. Audoin).

0041-624X/$ - see front matter © 2009 Elsevier B.V. All rights reserved.
doi:10.1016/j.ultras.2009.09.019

signals. It is used in Section 4 to comment on the maximum temperature rise in the cell and the maximum stress applied at the cell–substrate interface. Repetitive measurements, achieved on two species of a same cell variety, illustrate the sensitivity and the reproducibility of the measurements. Finally, the potentialities for cell imaging with a micron lateral resolution are shown in Section 6 of this paper.

2. Opto-acoustic generation in a single cell

Experiments mentioned in this paper are achieved with allium cepa (common onion) cells. Slices of alive cells are deposited directly on the surface of a polished titanium alloy (Ti6Al4 V) substrate. The thickness and the lateral size of a cell are measured by optical microscopy as approximately ~5 μm and 50–100 μm, respectively. All the experiments are performed at the room temperature of 21 °C without any treatment or fixation of the alive cells.

Well known reflectometric pump–probe experimental set-up is used [1] to generate and detect acoustic waves in the cells. The radiation of a femtosecond laser (wavelength 790 nm, mean power 1 W, pulse duration 100 fs, energy of the pulse 10 nJ) is divided to provide the pump and probe beams. The pump beam is modulated at a frequency of 330 kHz to provide a reference signal for lock-in amplification. Pump pulses are frequency-doubled (395 nm) through a BBO crystal. In our experiments, the pump beam mean power is reduced to 50 μW, hence to an energy of 0.5 pJ per pulse. An optical delay line (0–12 ns) is introduced in the probe beam path. Intensity of the reflected probe beam is detected by a photodiode. Such a set-up allows the detection of reflectivity relative variations at a level as low as 10^{-7}. Note that pump and probe wavelengths can be exchanged, thus providing either blue or red light for each of them. Both beams are focused at the cell–substrate interface by a same objective with a 50× magnification. The width at mid-height of the space cross-correlation of the pump and probe beams is approximately 2 μm.

Absorption of the pump laser beam in the substrate provides a local change of the temperature, which induces thermal and acoustic strains. The so generated sound pulse propagates with longitudinal sound velocity in the cell and in the substrate. The space profiles of the acoustic pulses are mainly determined by the optical penetration depth in the absorbing substrate, typically 10 nm for metals.

The acoustic contribution to the reflectivity changes measured at a same location within a vegetal cell with either blue (λ = 395 nm) or red (λ = 790 nm) probe light are shown in Fig. 1. Oscillations, revealing acoustic contributions at 11 GHz and 5.5 GHz, respectively, are detected with a very good signal to noise ratio. The nature of these oscillations will be discussed in the following section.

3. In silico

In this section, the opto-acoustic wave generation and detection in the cell are simulated. The model couples the temperature diffusion equation and the wave motion equation. Finally, the reflectivity changes are calculated accounting for both the temperature rise and the acoustic strain.

The cell and substrate are modeled as two infinite half spaces in contact at the plane $z = 0$, with the z axis oriented toward the depth of the substrate. In the following, index $i = 1, 2$ refers to the cell ($z < 0$) and to the substrate ($z > 0$), respectively.

Assuming no light absorption in the cell, the heat sources brought by light absorption in the media are

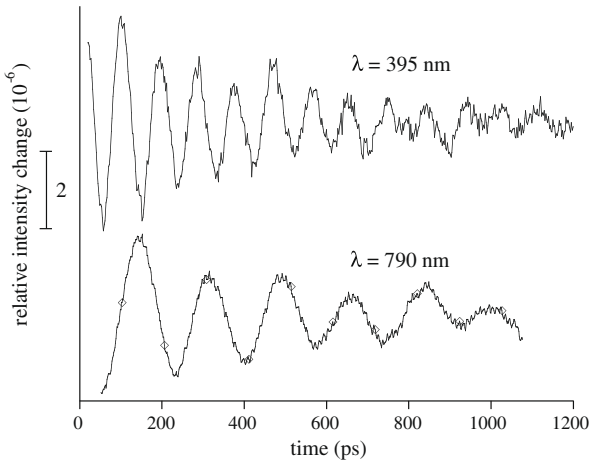

Fig. 1. Acoustic signals measured at a same position within a cell for probe light at λ = 395 nm (top), and λ = 790 nm (bottom).

$$\begin{cases} Q_1(z,t) = 0 \\ Q_2(z,t) = \beta_2 I_2 \delta(t) e^{-\beta_2 z} \end{cases} \quad (1)$$

where β_2 stands for the optical absorption coefficient, $I_2 = I_1(1 - R_{12})$ with R_{12} the reflection coefficient at the cell–substrate interface and I_1 the laser pulse fluence in the cell. Owing to the high transmission at the cell surface, I_1 can be considered equal to the incident laser fluence per pulse.

The temperature fields $T_i(z,t)$ comply with the heat diffusion equations

$$\rho_i C_{pi} \frac{\partial T_i(z,t)}{\partial t} - \kappa_i \frac{\partial^2 T_i(z,t)}{\partial z^2} = Q_i(z,t) \quad (2)$$

where ρ_i, C_{pi} and κ_i denote the mass densities, specific heat capacities and thermal conductivities, respectively. Since no heat source exists in the cell, the temperature rise in this medium results of the temperature and heat flux continuities at the cell–substrate interface. For a correct representation of the interface, thermal resistivity is introduced in the boundary equation as

$$T_2(0,t) - T_1(0,t) = R\Phi_i \quad (3)$$

with Φ_i the heat flux at the interface.

The sudden heating of the media generates transient acoustic displacements $u_i(z,t)$. They are solutions of the wave propagation equations

$$C_i \frac{\partial^2 u_i(z,t)}{\partial z^2} - \rho_i \frac{\partial^2 u_i(z,t)}{\partial t^2} = \lambda_i \frac{\partial T_i(z,t)}{\partial z} \quad (4)$$

where C_i and λ_i are the stiffness coefficients and the thermal rigidity coefficients, respectively. To account for sound attenuation in the media complex stiffness coefficients are considered. The displacements are such that continuity of the stress

$$\sigma_i(z,t) = C_i \frac{\partial u_i(z,t)}{\partial z} - \lambda_i T_i(z,t) \quad (5)$$

is satisfied at the interface ($z = 0$).

At this stage, one should remind that the physical data of experimental access are the relative changes of the probe light intensity. In the following, the acousto-optic interaction in the substrate is neglected. Let $f(z)$ denote the intensity change caused by a perturbation of the optical index at position z. The principle of the optical detection of the strain pulse is shown in Fig. 2. Owing to the acousto-optic interaction in the cell, a part of the electromagnetic wave is propagated backward to the detector (beam (a) in Fig. 2). The remaining electromagnetic energy is reflected at the cell–substrate